sustainability

MDPI

Article

Hydrothermal Liquefaction of Pinewood Sawdust: Influence of Reaction Atmosphere

Haoyu Wang [1], Yipei Jiang [1], Evan Park [1], Xue Han [2], Yimin Zeng [2,*] and Chunbao Xu [1,*]

[1] Department of Chemical and Biochemical Engineering, Western University, London, ON N6A 5B9, Canada; hwang928@uwo.ca (H.W.); yjian243@uwo.ca (Y.J.); epark225@uwo.ca (E.P.)
[2] CanmetMATERIALS, NRCan, Hamilton, ON L8P 0A5, Canada; xue.han@nrcan-rncan.gc.ca
* Correspondence: yimin.zeng@nrcan-rncan.gc.ca (Y.Z.); cxu6@uwo.ca (C.X.)

Abstract: Hydrothermal liquefaction (HTL) is a thermochemical process for production of biocrude oils, commonly from wet biomass under inert atmosphere (N_2). Influence of reaction atmosphere on HTL of pinewood sawdust was investigated in this work, at 300 °C for 60 min with the presence of KOH or H_2SO_4 catalyst under N_2, H_2, and O_2 atmosphere, respectively. Very interestingly, the reaction atmosphere showed significant influence on both products distribution and properties of the biocrude oils. Generally, H_2 atmosphere enhanced biomass degradation in the presence of either KOH or H_2SO_4 catalyst, producing the highest biocrude oil yield, lowest solid residue yield, and the best oil quality in terms of total acid number (TAN), viscosity and average molecular weights (Mn, Mw). Whereas the HTL in O_2 atmosphere showed the poorest performance in terms of yields and properties of biocrude oils. The highest quality of biocrude oil was produced using KOH catalyst in H_2 atmosphere with the maximum biocrude yield (approx. 34 wt.%) and the highest energy recovery (ER) in biocrude (ER = 73.14%). The measured properties of the oil are as follows: TAN = 40.2 mg KOH/g, viscosity = 51.2 cp, Mn = 470 g/mol, Mw = 767 g/mol. In addition, the biocrude oils produced in H_2 atmosphere contain more light oil (naphtha) fraction (23.9 wt.% with KOH and 16.5 wt.% with H_2SO_4) with lower boiling points, while those generated in O_2 atmosphere have more carboxylic acid compounds.

Keywords: reaction atmosphere; biocrude properties; KOH; hydrogen; H_2SO_4; hydrothermal liquefaction; nitrogen; oxygen; pinewood sawdust; products distribution

Citation: Wang, H.; Jiang, Y.; Park, E.; Han, X.; Zeng, Y.; Xu, C. Hydrothermal Liquefaction of Pinewood Sawdust: Influence of Reaction Atmosphere. *Sustainability* **2023**, *15*, 6698. https://doi.org/10.3390/su15086698

Academic Editor: Francesco Nocera

Received: 16 March 2023
Revised: 6 April 2023
Accepted: 9 April 2023
Published: 15 April 2023

1. Introduction

The growing energy demand has led to extensive use and overexploitation of fossil resources, resulting in an energy crisis and severe environmental issues such as climate changes [1–3]. To mitigate the pressure from the global energy shortage and global warming due to fast increased CO_2 emission, as well as to satisfy the clean energy demand, sustainable development and carbon neutrality, biomass has gained immense interest for the production of energy, fuels, chemicals and materials [4,5]. Biomass is a renewable and abundantly available resource from dedicated energy crops or various organic wastes, such as wood and forestry residues, agricultural crops and crop residues, marine products, wastewater sludge, microalgae, etc. [6–8].

Biomass can be converted into energy, fuels and chemicals via biochemical and thermochemical technologies. Biochemical treatments mainly refer to anaerobic digestion, fermentation, and photobiological hydrogen production. The objective of these treatments was to utilize various microorganisms or enzymes to convert the biomass into a variety of products and intermediates. This process offers an opportunity to produce an assortment of fuels and chemicals, including biogas, hydrogen, ethanol, butanol, acetone, and various organic acids [9]. However, biochemical processes are very sensitive to operating conditions (such as pH, temperature, and residence time) and quite slow (usually requiring days or

weeks to complete). [10–12]. Thermochemical processes include gasification, hydrothermal liquefaction (HTL), pyrolysis, and combustion [13,14]. Pyrolysis and HTL are two main thermochemical pathways developed for the transformation of raw biomass materials into liquid products that can be further processed to produce biofuels or bio-based chemicals. Compared with pyrolysis, HTL has gained increasing attention because it can produce high quality biocrude oils (5–20% oxygen) as the primary products with little gas generated [15]. More advantageously, HTL can handle wet feedstocks (with >70% water content) without the requirement for drying [13,16], and it typically operates in an inert atmosphere (N_2) at milder temperatures (250–400 °C), though under high pressure (50–250 bar) [6,17,18].

Many studies focus on the effects of HTL process parameters, e.g., reaction temperature, pressure, residence time, and types of solvent. Generally, operations at a moderate temperature between 250–350 °C obtain a higher biocrude yield; too high temperature would reduce bio-crude yield and increase the amount of solid residue due to bio-oil cracking and the repolymerization/condensation of cracking intermediates [16,19–21]. Shortening residence time can prevent these reactions happening to a certain extent, resulting in an increased biocrude yield. However, a too-short duration would cause incomplete biomass degradation [22]. A lower biomass-to-solvent ratio increased the yield of biocrude and inhibited the formation of solid residues and gases owing to better dissolution of reaction intermediates/products in the solvent (water or a mixture of water and organic solvent) and the enhanced hydrolysis reactions of the biomass [23]. Catalyst is another critical factor that affects HTL biocrude yield and properties. Homogeneous catalysts, including soluble acids, bases, and alkali salts, are commonly used in biomass HTL. Strong acids (sulfuric acid and hydrochloric acid) exhibited great performance in biomass conversion. However, strong acids could corrode the experimental equipment, and the biomass conversion might decrease when increasing the acid content over a certain level [24,25]. In addition, acidic condition facilitates the condensation and re-polymerization reactions of the reaction intermediates, thereby reducing the yield of biocrude. Alkaline catalysts such as NaOH, K_2CO_3, KOH, and Na_2CO_3 have been widely used in HTL processes [14]. Alkaline catalysts can neutralize the acid compounds in the hydrothermal products, which prevents the repolymerization/condensation of the reaction intermediates, thus reducing the formation of solid residue/char [26]. Recently, researchers have employed mathematical models to optimize the parameters of HTL of biomass. The goal of this optimization is to obtain biocrude with high yield, high carbon and hydrogen content, and low heteroatom content, along with the corresponding reaction conditions and material composition. The primary methods include empirical summaries based on experimental laws, response surface method (RSM), kinetics modeling, and machine learning (ML). For example, Zhu et al. [27] utilized RSM to optimize reaction temperature, reaction time, catalyst dosage and biomass/water ratio for highest bio-oil yield. Obeid et al. [28] employed kinetics modeling to predict the distribution of biocrude yield. Cheng et al. [29] used multiple linear regression (MLR), regression tree (RT) and random forest (RF) to predict the quantity and quality of biomass HTL products.

However, few studies reported the effects of the reaction atmosphere on biomass HTL with respect to the products distribution and properties of the biocrude. HTL of biomass is typically operated in an inert atmosphere, usually pressurized nitrogen, to avoid boiling of the reaction mixtures. Zhang et al. found that using a reducing gas (CO, H_2) as the HTL reactor pressurizing gas could inhibit condensation, cyclisation, and re-polymerization of free radicals of the reaction intermediates, and hence stabilize the depolymerized lignocellulose fragments and reduce char formation [30]. Yin et.al reported that using CO or H_2 as the reaction atmosphere in HTL of cattle manure led to increased biocrude production by 5–15 wt.% [31]. Interestingly, Yin et al. also tested oxygen as an oxidative atmosphere for cattle manure HTL, resulting in much lower biocrude yield compared with those obtained under N_2 or CO atmosphere, due to the oxidation of feedstocks/products in the presence of an excess of oxygen in the reactor [31]. In another research by Rahimi et al. in HTL conversion of lignin, oxygen atmosphere was found

to promote the cleavage of alkyl aryl ether units in lignin to yield low molecular weight compounds such as vanillin and benzylic/aliphatic alcohols [32,33].

Lignocellulosic biomass is one of the most commonly used feedstocks for HTL process. However, no research has indicated which atmosphere (inert, oxidative, or reductive) works best for the HTL conversion of lignocellulosic biomass. In this study we for the first time compared the oil product yield and properties from HTL of a typical lignocellulosic biomass-pinewood sawdust—under different reaction atmospheres (N_2, H_2, and O_2) on HTL of a typical lignocellulosic biomass-pinewood sawdust. The tests were conducted with a biomass-to-water ratio of 1:15 (*w*/*w*) at 300 °C for 60 min under N_2, H_2, or O_2 atmosphere in the presence of a homogeneous catalyst: KOH or H_2SO_4. The biocrude products were comprehensively characterized for their physicochemical properties, i.e., viscosity, total acid number (TAN), functional groups by Fourier-transform infrared spectroscopy (FT-IR), volatile compositions by gas chromatography-mass spectrometry (GC-MS), volatility by thermogravimetry analysis (TGA), and average molecular weights and distributions by gel permeation chromatography (GPC).

2. Materials and Methods

2.1. Materials

Pinewood sawdust was collected from a local sawmill (London, ON, Canada). Prior to the HTL tests, it was crushed and sieved to reduce particle size below 0.3 mm, followed by pre-drying at 105 °C in an oven for 24 h. It contains 40.9 wt.% cellulose, 28.5 wt.% hemicellulose and 28.4 wt.% lignin. Its proximate analysis and ultimate analysis, were obtained from our previous work [34], as shown in Table 1. Potassium hydroxide (KOH, 99 wt.%) and sulfuric acid (H_2SO_4, 98 wt.%) were purchased from Sigma-Aldrich (Oakville, ON, Canada), and VWR International (Mississauga, ON, Canada), respectively. Reagent-grade acetone (99.5 wt.%) was purchased from Fisher Scientific (Ottawa, BC, Canada). De-ionized water was used as the solvent in HTL experiments.

Table 1. Proximate analysis and ultimate analysis of the pinewood sawdust feedstock.

Proximate Analysis (wt.%) [a]	
Volatile matter (VM)	85.35 ± 0.99
Fixed carbon (FC)	14.02 ± 0.92
Ash	0.63 ± 0.07
Elemental analysis (wt.%) [a]	
C	48.24 ± 0.82
H	4.72 ± 0.12
O [b]	46.33 ± 0.76
N	0.08 ± 0.01
S	n.d. [c]
HHV(MJ/kg) [d]	14.78

[a] On dry basis; [b] Calculated by difference: %O = 100% − C% − H% − N% − S% − Ash%; [c] Not detected; [d] Higher heating value, calculated by Dulong equation [HHV (MJ/kg) = 0.338C + 1.428(H-O/8) + 0.095S].

2.2. Apparatus and Methods

2.2.1. HTL Experiments

The HTL experiments were conducted in a 100 mL Parr 4590 autoclave batch reactor (made of SS 316L) equipped with a stirrer and temperature controller. In a typical HTL run, 2 g of pinewood sawdust together with 30 g de-ionized water (solid-to-liquid ratio is fixed as 1:15 *w*/*w*) were loaded into the reactor. The catalyst (KOH or H_2SO_4) dosage was set to be 5 wt.% with respect to the mass of dry biomass feedstock. The reactor was sealed, and the air inside was displaced by vacuuming and purging for three times with N_2, H_2, or O_2, followed by pressurizing the reactor to 2 MPa using N_2, H_2, or O_2. Then the reactor was heated under 100 rpm stirring at approx. 10 °C/min to 300 °C and maintained at the temperature for 60 min for reaction, followed by quenching in a water bath.

2.2.2. Products Separation

The products from the HTL experiments include gaseous products, biocrude oil, aqueous-phase (AP) products, and solid residues (SR). After the reactor was quenched to room temperature, the gas products from HTL were vented into a gas bag and analyzed by Micro-GC-TCD (Agilent 3000). The gas products composition (mainly CO_2) was used for calculation of mass of gas products, M_{gas}. Then the reactor was opened and the solid/liquid products inside the reactor were first washed out with distilled water. The resulting suspension was filtered under vacuum through a pre-weighted VWR No. 413 filter paper. The reactor was then further washed with reagent-grade acetone to collect the water-insoluble oil components. The mixture was filtered under vacuum through the same filter paper (VWR No. 413) retaining the solid residue on it. The solid residue or char was rinsed with additional acetone until the filtrate became colorless, followed by oven dried at 105 °C until attaining a constant weight to determine the mass of solid residue (M_{SR}). The filtrate was evaporated under reduced pressure at 50 °C until bio-crude oil was precipitated on the flask inner wall. The remaining aqueous solution was decanted and collected as the aqueous product (AP). The oily product sticking on the flask, designated as biocrude oil or simply bio-oil, was weighed to determine the mass of biocrude, $M_{biocrude}$. The yields of the HTL products were calculated based on dry and ash-free mass of biomass feedstock, $M_{Biomass,daf}$, as follows:

$$Biocrude\ yield(wt.\%) = \frac{M_{biocrude}}{M_{Biomass,daf}} \times 100 \quad (1)$$

$$SR\ yield(wt.\%) = \frac{M_{SR}}{M_{Biomass,daf}} \times 100 \quad (2)$$

$$Gas\ yield(wt.\%) = \frac{M_{gas}}{M_{Biomass,daf}} \times 100 \quad (3)$$

$$AP\ yield(wt.\%) = 100 - Biocrude\ yeild - SR\ yield - Gas\ yield \quad (4)$$

$$Energy\ recovery(\%) = \frac{HHV_{biocrude}}{HHV_{Biomass}} \times Biocrude\ yield \quad (5)$$

2.2.3. Products Analysis

The composition of the collected gaseous products in the gas bag was analyzed with a Micro-GC-TCD (Agilent Micro-GC 3000) by injecting 50 mL of air as the internal standard. A PerkinElmer Fourier transform infrared spectrometer (FT-IR, MA, USA) was used to determine the functional groups of the biocrude products. The biocrude viscosity at 80 °C was measured using a Brookfield CAP 2000 + Viscometer. The weight/number average molecular weights (Mw, Mn), polydispersity index (PDI, =Mw/Mn), of the obtained biocrude products were determined by Gel Permeation Chromatography (GPC-UV, Waters Breeze). Volatile compositions of the biocrude products were analyzed by Gas Chromatograph-Mass Spectrometer (GC–MS, Agilent Technologies, 5977A MSD, Santa Clara, CA, USA) equipped with an HP-5MS column (30 m × 250 μm × 0.25 μm). The GC temperature program was set as: held at 40 °C for 5 min, then increased at 10 °C/min to 150 °C and held for 2 min, increased at 10 °C/min to 290 °C and held for 5 min. The elemental compositions (C, H, N, and S) of the biomass feedstock and biocrude products were analyzed on an elemental analyzer (Vario EL Cube). The O content was calculated by difference on a dry basis (%O = 100% − %Ash − %C − %H − %N − %S) where the ash content was determined by ashing at 700 °C for 4 h in a muffle furnace. The higher heating values (HHV) of the biomass feedstock, bio-crude oils, and solid residue were calculated by Dulong equation [HHV (MJ/kg) = 0.338C + 1.428(H-O/8) + 0.095S]. The proximate analysis (volatile matters and fixed carbon contents) of biomass feedstock and biocrude products

was determined on a thermogravimetric analyzer (Pris 1 TGA, Waltham, MA, USA), where the sample was heated in 30 mL/min N_2 flow from 25 °C to 800 °C at 10 °C /min, followed by soaking at this temperature for 15 min in 30 mL/min air flow for ashing. The total acid number (TAN) of biocrude was determined by titration on a pH meter (Titroline 7000) using 0.01 N KOH and phenolphthalein as the titration solution and indicator, respectively. TAN was calculated in milligrams of KOH/gram of the biocrude sample as follows:

$$TAN = [(A - B)N \times 56.1]/W \quad (6)$$

where:

A = KOH solution required for titration of the sample, mL,
B = KOH solution required for titration of the blank, mL,
N = Normality of the KOH solution,
W = Mass of the biocrude sample, g.

3. Results and Discussions

3.1. HTL Products Distribution

Figure 1 shows the products distribution in HTL of pinewood sawdust under N_2, H_2, and O_2, respectively, with KOH or H_2SO_4 catalyst. As clearly shown in the Figure, reaction atmosphere and catalyst both have significant influence on the products distribution in HTL of the woody biomass. In terms of biocrude yield and SR yield, the alkali catalyst (KOH) outperformed the acid catalyst (H_2SO_4), and H_2 atmosphere was superior to both N_2 and O_2. The highest biocrude yield (approx. 34 wt.%.) and maximum biomass conversion (approx. 91%, or SR~9 wt.%) was achieved under the H_2 atmosphere with KOH catalyst. In contrast, the presence of O_2 atmosphere with KOH catalyst produced the lowest biocrude yield (approx. 2 wt.%) and minimum biomass conversion (approx. 63%, or SR~37 wt.%).

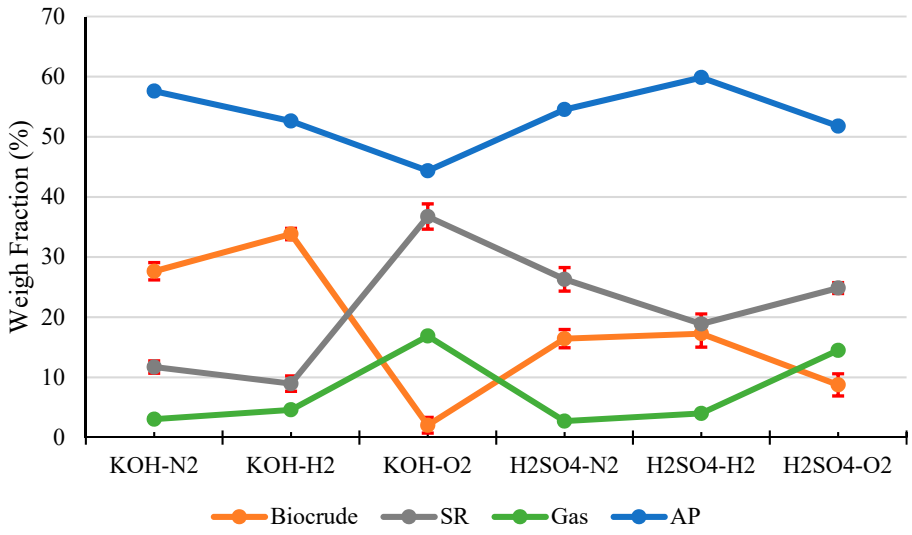

Figure 1. Products distribution from HTL of pinewood sawdust at 300 °C for 60 min under N_2, H_2, and O_2, respectively, with KOH or H_2SO_4 catalyst.

Pinewood sawdust is a typical woody biomass contains 60–70 wt.% holocellulose (cellulose and hemicellulose), 20–30 wt.% lignin, and 5–10 wt.% others (extractives and ash) [35]. Holocellulose includes polysaccharides with β(1→4) linkage [36], and lignin is a well-known polymer of phenylpropane linked mainly by β-O-4 ether linkage. During HTL, the β(1→4) linkage in holocellulose, and β-O-4 ether linkage in lignin can be broken via hydrolytic depolymerization, forming carbohydrate/phenolic monomers and oligomers as HTL reaction intermediates, which would further undergo recombination reactions to form biocrude components including organic acids and phenolics [37]. The hydrolytic depolymerization process could be catalyzed by acid catalyst or self-catalyzed by the

organic acids formed in the biomass HTL process. However, the acid catalyst could catalyze the condensation/repolymerization, decarboxylation and dehydration reactions of the HTL reaction intermediates to form SR product [38,39], whereas an alkaline catalyst, e.g., KOH can neutralize the organic acids produced and inhibit condensation/repolymerization reactions [15], hence restricting SR yield and improving biocrude yield, which explains the results in Figure 1.

On the other hand, the reaction atmosphere exhibits a significant influence on the HTL products distribution. First of all, the H_2 atmosphere could play positive roles in breaking of the β(1→4) linkage in holocellulose and β-O-4 ether linkage in lignin via reductive depolymerization and stabilizing the reaction intermediates [40], which would hence suppress the condensation/repolymerization reactions, restrict SR formation and improve biocrude yield, as evidenced by the results of this study (Figure 1). In contrast, under O_2 atmosphere, the reaction intermediates are converted into more carboxylic compounds that promote the formation of SR product, accompanied by significantly reduced yields of biocrude (Figure 1). More gaseous products were generated under O_2 atmosphere. Further analysis of the gas products indicates that the amount of produced CO_2 in O_2 atmosphere is much higher than those in N_2 or H_2 (Table 2), as a result of the enhanced decarboxylation and deep oxidation of the intermediates by O_2. In addition, the reductive environment (H_2) somewhat limits the production of CO_2. In a summary, among all three types of gas atmosphere examined, biomass HTL under H_2 atmosphere showed the highest biocrude yields and the lowest SR yields. It is worth noting that although an inert atmosphere (N_2) exhibited an average performance in terms of biocrude yield and biomass conversion, N_2 is more economical and safer than H_2 and O_2, hence has been employed most often for biomass HTL.

Table 2. Yield of gas products obtained from HTL of pinewood sawdust at 300 °C for 60 min under N_2, H_2, and O_2, respectively, with KOH or H_2SO_4 catalyst.

Yield of Each Gas Species (mmol/g)	Catalyst: KOH			Catalyst: H_2SO_4		
	N_2	**H_2**	**O_2**	**N_2**	**H_2**	**O_2**
H_2	0.0612	-	0.0083	0.0662	-	0.0419
CH_4	0.0051	0.0024	0.0058	0.0019	0.0045	0.0103
CO	0.0818	0.1257	0.0301	0.0951	0.3487	0.1074
CO_2	0.6196	0.5562	3.7920	0.5628	0.3834	0.9146
C_2H_4	0.0004	0.0002	0.0006	0.0002	0.0011	0.0006

3.2. Properties of Biocrude Products

Table 3 presents the results of the elemental compositions, HHV, viscosity, average molecular weights, and TAN of the obtained biocrude oils from HTL of pinewood sawdust at 300 °C for 60 min under N_2, H_2, and O_2, respectively, with KOH or H_2SO_4 catalyst. In terms of elemental compositions of the biocrude products, the effects of catalyst type were minimal, but the atmosphere showed significant influence on elemental compositions and all other oil properties. Generally, the biocrude oils obtained under N_2 or H_2 atmosphere have a better quality than those obtained under O_2 atmosphere: a higher H/C ratio, lower O/C ratio, higher HHV, lower TAN, much lower viscosity and much smaller M_n and M_w. HTL operations under N_2 or H_2 atmosphere also led to much higher energy recovery (65–73% with KOH catalyst and 35–42% with H_2SO_4 catalyst) than those under O_2 atmosphere (approx. 3% with KOH catalyst and 16% with H_2SO_4 catalyst). The HTL experiment using KOH catalyst under H_2 achieved the best energy recovery (ER~73%) owing to the highest biocrude production yield (~34 wt.%) obtained under these conditions. Although surprisingly the H/C ratios of the biocrude oils obtained under H_2 atmosphere are smaller than those of the oils obtained under N_2 (suggesting more condensed structure of the oils, whose causes require future research), the oils obtained under H_2 atmosphere have better properties: lower TAN, much lower viscosity and smaller Mn and Mw. Apparently, the biocrude oils from the HTL experiments under H_2 atmosphere are much less viscous and

have smaller molecular mass than the oils obtained under N_2 or O_2 atmosphere, which could be attributed to reductive depolymerization of holocellulose and lignin, as well as hydrocracking reactions. These reactions would result in breakage of the C-O-C and C–C bonds of the complex macromolecular structure of biomass substrate/intermediates into simpler small-molecule substances [41], and hence a reduced viscosity of the biocrude products. Compared with the average molecular weight of the Illinois shale oil (M_w = 670 g/mol, M_n = 270 g/mol) [42], the biocrude oils from the HTL still have larger average molecular weights (M_w = 654–1347 g/mol, M_n = 417–753 g/mol), because deep-depolymerization of lignocellulose is very difficult under testing conditions due to the unavoidable occurrence of self-condensation and repolymerization reactions during the conversion process [43].

Table 3. Properties of biocrude products from HTL of pinewood sawdust at 300 °C for 60 min under N_2, H_2, and O_2, respectively, with KOH or H_2SO_4 catalyst.

	Catalyst: KOH			**Catalyst: H_2SO_4**		
	N_2	**H_2**	**O_2**	**N_2**	**H_2**	**O_2**
Ultimate analysis [a] (wt.%)						
C	72.95	72.44	51.83	72.22	71.52	69.75
H	5.86	4.63	2.95	5.55	3.78	3.18
N	0.16	0.05	0.21	0.08	0.06	0.08
S	n.d. [c]	n.d. [c]	n.d. [c]	n.d. [c]	n.d. [c]	n.d. [c]
O [b]	21.03	22.84	45.01	22.15	24.64	27.00
O/C	0.22	0.24	0.65	0.23	0.26	0.29
H/C	0.96	0.77	0.68	0.92	0.63	0.55
HHV [d] (MJ/kg)	29.27	27.01	13.69	28.38	25.17	23.29
ER [e] (%)	64.76	73.14	2.81	41.91	34.81	16.34
Viscosity @ 80 °C, (cp)	84.1	51.2	113.6	86.4	64.4	109.7
TAN (mg KOH/g oil)	45.7	40.2	131.3	118.4	86.6	148.3
M_n (g/mol)	504	470	753	457	417	704
M_w (g/mol)	815	767	1347	721	654	1226
PDI	1.62	1.63	1.75	1.58	1.57	1.74

[a] On dry basis; [b] Calculated by difference %O = 100% − C% − H% − N% − S% − Ash%; [c] Not detected; [d] Calculated by Dulong equation; [e] Obtained by Equation (5).

The M_w and M_n of the biocrude oils from the experiments with KOH catalyst are slightly higher than those with H_2SO_4 catalyst. This result might be owing to the acid-catalyzed cleavage of alkyl-aryl ether linkages, e.g., β-O-4 linkage, in lignin, as well as the acid-catalyzed breakage of the 1,4′-β-glycosidic bonds (β(1→4) linkage) in holocellulose [44]. Moreover, compared with oils obtained with KOH catalyst, the oils obtained with H_2SO_4 catalyst are more acidic, especially for those obtained under O_2 atmosphere (with a greater TAN), suggesting the presence of more organic acids, which can be confirmed by the GC-MS analysis results as discussed below.

The volatile compounds of the bio-crude oils were analyzed by GC-MS. The results are shown in Figure 2. The identified compounds include carboxylic acids, alcohols, aldehydes, aromatics, esters, ethers, hydrocarbons, ketones, nitrogenous compounds, and phenols. The main volatile compounds in the oils obtained under N_2 or H_2 atmosphere with KOH catalysts are phenols and aromatic compounds, and the oils obtained under H_2 atmosphere contain more phenols than those obtained under N_2 atmosphere, likely owing to the reductive depolymerization of lignin [40,45]. In comparison to oils obtained under N_2 or H_2 atmosphere with KOH catalyst, the biocrudes obtained with H_2SO_4 catalyst contain much more carboxylic acids and ketones, suggesting acid-catalyzed degradation of cellulose and hemicellulose structures [46].

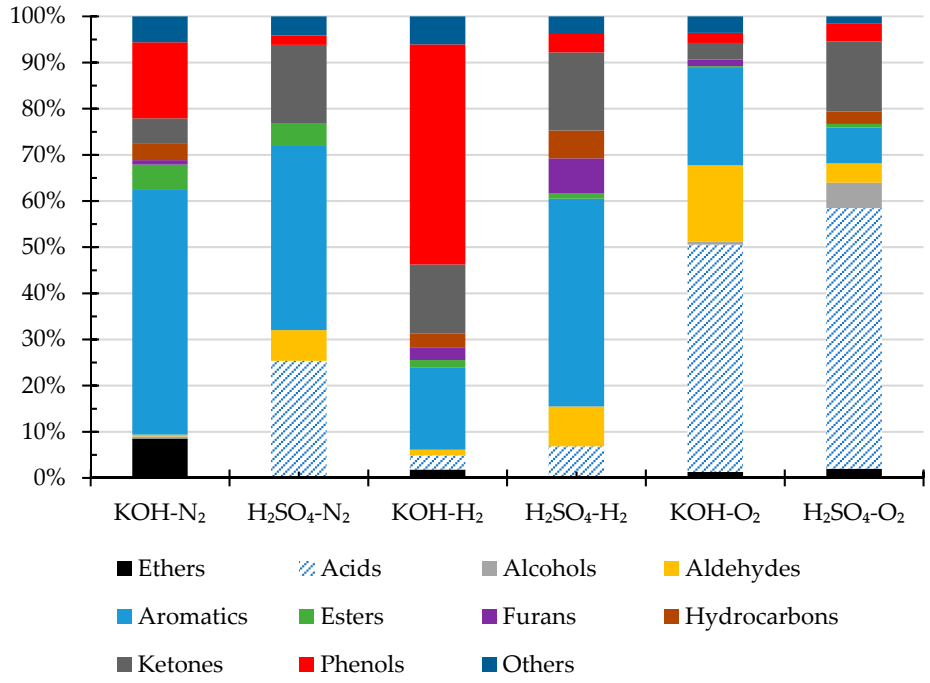

Figure 2. Volatile compositions (area% by GC-MS) of the biocrude products from HTL of pinewood sawdust at 300 °C for 60 min under N_2, H_2, and O_2, respectively, with KOH or H_2SO_4 catalyst.

More interestingly, the oils from the HTL experiments under O_2 atmosphere contain much more acids than those obtained under H_2 or N_2. Estimated by the area %, the oils obtained under O_2 atmosphere with KOH or H_2SO_4 catalyst contain approx. 41% and 56% of acids, respectively, corresponding to much higher TAN as evidenced in the results presented previously in Table 3. Under the oxygen atmosphere, phenols could deprotonate to form phenoxy radicals by electron transfer from oxygen and be stabilized by the resonance, resulting in the formation of carbonyl and carboxylic acid, and H_2SO_4 acid could also catalyze aromatic ring opening, leading to formation of pentatonic acids [47]. The detailed compounds in bio-crude oils were summarized in Table A1.

The functional groups of the biocrude oils were identified by FT-IR and the spectra are illustrated in Figure 3. The broad IR absorption at 3350 cm^{-1} is typical of O-H stretching, suggesting the presence of alcohols, phenols, carboxylic acids, or water residues in the oils. The absorbance at 1700 cm^{-1}, representing the C=O stretching vibration of carbonyl groups, indicates the presence of ketones, aldehydes, esters or carboxylic acids in the oils. The relatively medium-intense peaks at 1611 and 1495 cm^{-1} represent aromatic nuclei, indicating the presence of aromatic rings and their derivatives. The IR absorption bands between 3000 and 2840 cm^{-1} are attributed to C-H stretching vibrations, indicating the presence of alkyl C-H in the oils. The two absorption peaks at 1370 and 1456 cm^{-1} are attributed to the bending vibrations of methyl (-CH_3) and methylene (-CH_2) groups, respectively. The presence of C-H bonds indicates the alkane groups in the biocrude oils. The bands between 1280 and 1000 cm^{-1} could be related to C-O vibrations, suggesting that the oils may contain acids, phenols, furans, or alcohols. The presence of the peak at 860 cm^{-1}, attributed to C-H bending, suggests the possible presence of single, polycyclic, and substituted aromatics. In the oils obtained under O_2 atmosphere, more oxygen containing compounds were produced in the biocrude oils, evidenced by the intensive peaks representing O-H, C=O and C-O bonds, compared to those of the oils obtained under N_2 or H_2 atmosphere. In addition, the intensities of aromatic absorptions at 1611 and 1495 cm^{-1} are weaker in the biocrudes obtained when using H_2SO_4 catalyst, especially under O_2 atmosphere, suggesting that the presence of oxidative agents (i.e., H_2SO_4 and O_2) could possibly restrict the aromaticity of reaction intermediates derived from lignin in pinewood.

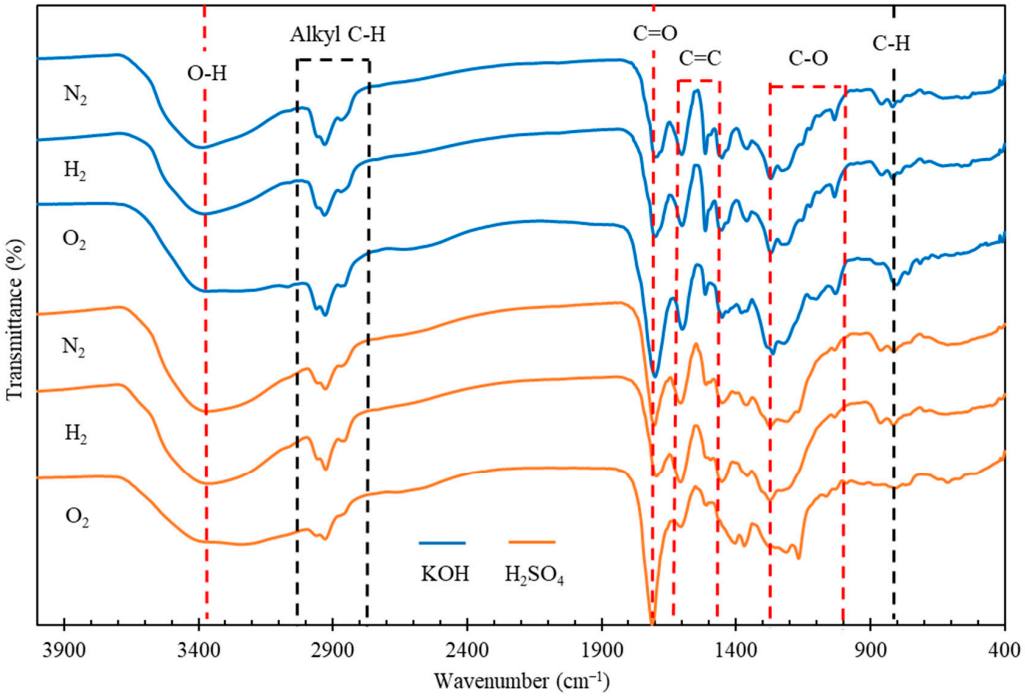

Figure 3. FT-IR spectra of biocrude products from HTL of pinewood sawdust at 300 °C for 60 min under N_2, H_2, and O_2, respectively, with KOH or H_2SO_4 catalyst.

Figures 4 and 5 illustrate the thermogravimetric (TG) and derivative thermogravimetric (DTG) curves, respectively, of the biocrude oils obtained under N_2, H_2, and O_2 with KOH or H_2SO_4 catalyst. The boiling point distributions of the oils, estimated from the TG curves, are presented in Table 4. The biocrudes obtained under N_2 and H_2 atmosphere had similar decomposition curves (TG). The initial decomposition of these biocrudes occurred at around 100–140 °C. Whereas, the decomposition of bio-oils from HTL of pinewood under O_2 started at around 160–180 °C. The distillate or volatile fractions of the oils (with a boiling point below 600 °C) obtained under N_2 and H_2 atmosphere vary from 59.21 wt.% to 67.26 wt.%, which fell in the range between North American tar sand bitumen (44–65 wt.% distillate) and the Venezuelan crude oil (66 wt.% distillate) [31,38]. However, the biocrudes produced under O_2 atmosphere are more thermally unstable with over 80 wt.% of volatile matters. Generally, the boiling point distributions of the oils obtained under N_2 and H_2 with KOH catalyst are similar, but the oil obtained under H_2 has a higher light fraction (<193 °C) (23.89 wt.%). The oils obtained under O_2 have more mild boiling fractions (343–538 °C) (55.85 wt.% with KOH catalyst, 35.43 wt.% with H_2SO_4 catalyst) and the least heavy residues fraction (>538 °C) (21.07 wt.% with KOH catalyst and 15.10 wt.% with H_2SO_4 catalyst).

The DTG peaks of the biocrude oils locate at two main temperatures ranges: from room temperature to 300 °C and from 300 °C to 450 °C (Figure 5). The weight loss from room temperature to 300 °C could be due to the evaporation of low molecular weight fractions in the oil samples. The major weight loss of all biocrude oil samples occurred between 300 °C and 450 °C. Interestingly, intensive weight loss peaks were observed between 100 °C and 200 °C in the oils obtained under the H_2 atmosphere, likely owing to the presence of more low molecular weight compounds (e.g., phenols) that evaporate in this temperature range, as confirmed by the GC-MS and GPC results discussed previously. The oils obtained under O_2 atmosphere are more thermally stable than those obtained under N_2 or H_2, with intensive weight loss peaks from 300 °C to 450 °C. In contrast, the DTG curves of the oils obtained under N_2 have flat and broad peaks across the entire temperature range.

Table 4. Boiling point distributions of the biocrude products from HTL of pinewood sawdust at 300 °C for 60 min under N_2, H_2, and O_2, respectively, with KOH or H_2SO_4 catalyst.

Distillate Range (°C)	Catalyst: KOH			Catalyst: H_2SO_4		
	N_2	H_2	O_2	N_2	H_2	O_2
<193 (Heavy Naphtha)	15.18	23.89	3.77	12.73	16.49	7.46
193–271 (Kerosene)	9.68	8.56	11.47	12.30	10.56	19.92
271–343 (Gas Oil)	8.27	11.64	7.84	11.56	9.28	22.09
343–538 (Vac. Gas Oil)	22.97	21.52	55.85	17.56	19.42	35.43
>538 (Residues)	43.90	34.39	21.07	45.85	44.25	15.10
VM [a] (wt.%)	59.98	67.26	81.53	60.35	59.21	85.71
Ash (wt.%)	n.d [b]	n.d [b]	n.d [b]	n.d [b]	n.d [b]	n.d [b]
FC [c] (wt.%)	40.02	32.74	18.47	43.34	30.79	14.29

[a] Volatile matter, calculated by summing fractions below 600 °C; [b] Not detected; [c] Fixed carbon, calculated by FC% = 100% − Ash% − VM%.

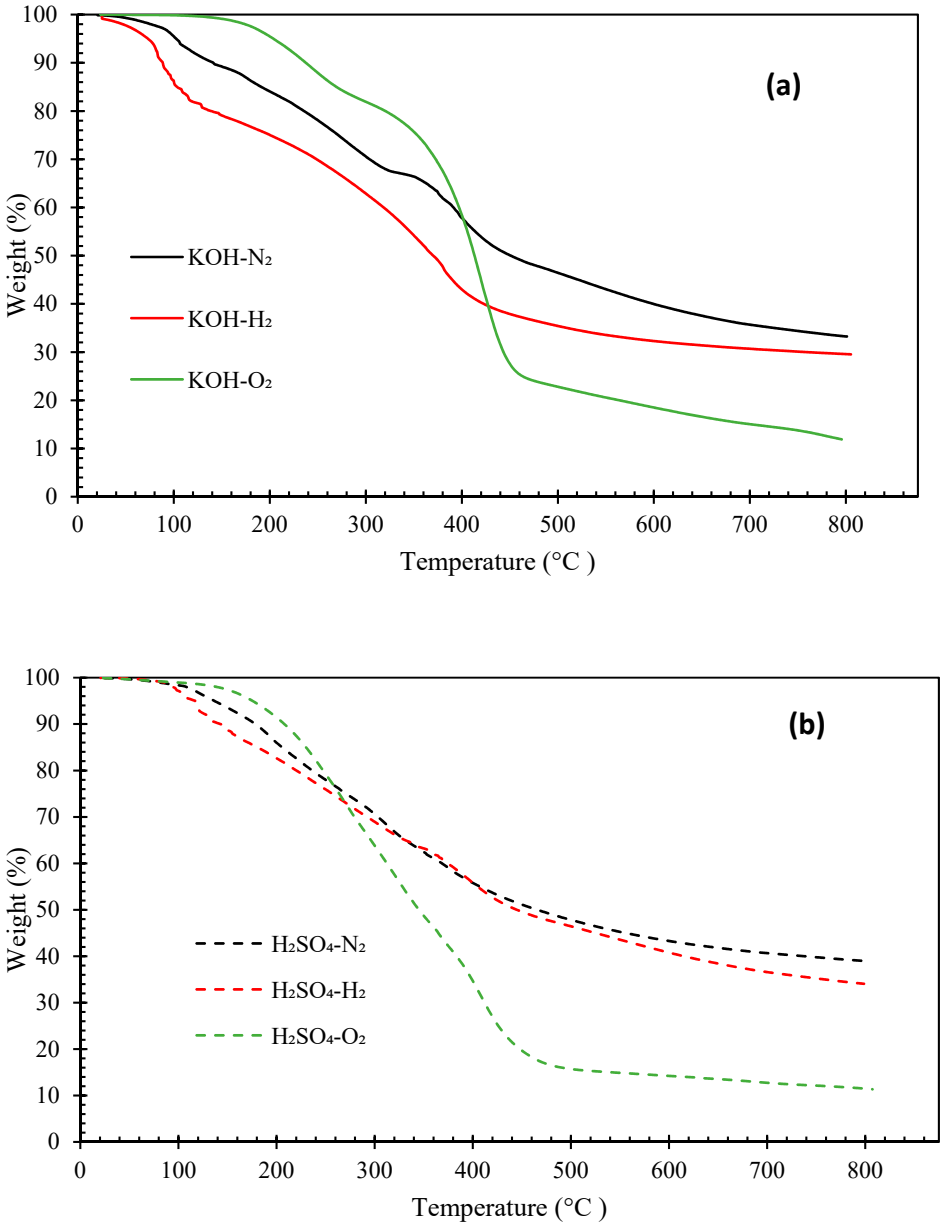

Figure 4. TG curves of biocrude products from HTL of pinewood sawdust at 300 °C for 60 min under N_2, H_2, and O_2, with KOH (**a**) or H_2SO_4 (**b**) catalyst.

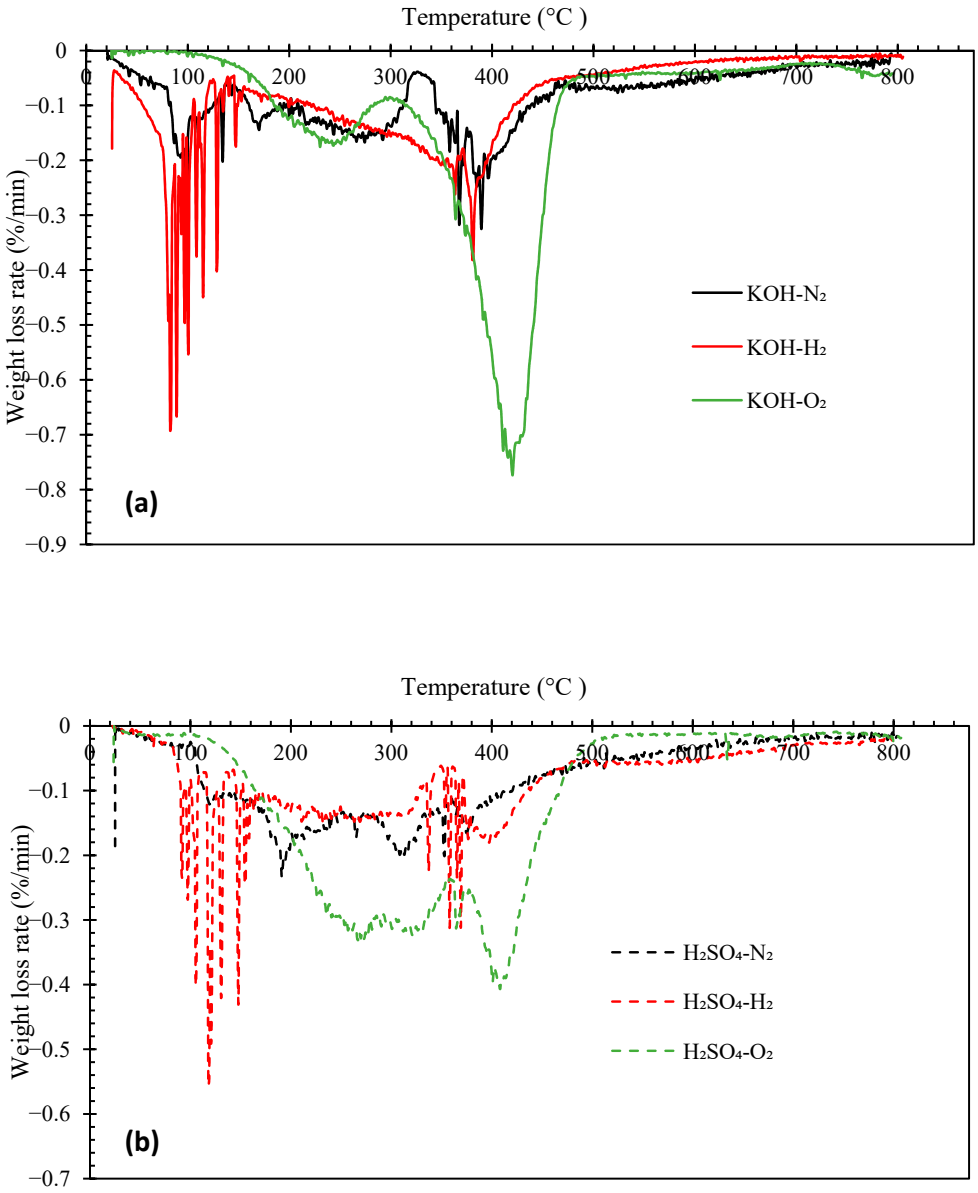

Figure 5. DTG curves of biocrude products from HTL of pinewood sawdust at 300 °C for 60 min under N_2, H_2, and O_2, with KOH (**a**) or H_2SO_4 (**b**) catalyst.

3.3. Economic Analysis

To perform a cost-benefit analysis of the HTL process, the costs and benefits associated with the process need to be considered, including capital investment (e.g., equipment and infrastructure, site development, engineering, etc.), operating costs (e.g., feedstock, labor, post-treatment, energy, maintenance, etc.), value of the produced oils, and environmental benefits. As mentioned above, the bio-oil produced under O_2 atmosphere has a higher oxygen content and average molecular weight compared to those obtained under N_2 and H_2 atmosphere and thus requires a much higher upgrading cost, including additional equipment, energy, and labor cost, to convert the biocrude into gasoline-like products. In addition, the significant lower bio-oil yield from pinewood HTL process under O_2 atmosphere will increase the feedstock and labor cost as well due to the more raw materials consumed and longer operating time required to achieve the aimed producing capacity. Besides, the higher TAN value of bio-oil obtained under O_2 will cause corrosion problem on core HTL equipment, which will increase the maintenance costs. Although biomass HTL under H_2 atmosphere showed the best biocrude yields and chemical properties, the safety issues accompanying H_2 will possibly cause additional operating cost (e.g., insurance,

training, etc.). Thus, N_2 has been employed most often for biomass HTL. A comprehensive and detailed techno-economic assessment will be carried out in the future research.

4. Conclusions

The study investigated the effect of reaction atmosphere on hydrothermal liquefaction (HTL) of pinewood sawdust using KOH or H_2SO_4 catalyst at 300 °C, 20 bar for 60 min under N_2, H_2, and O_2 atmospheres. The results showed that HTL under H_2 atmosphere with KOH catalyst led to the highest biocrude yield (approx. 34 wt.%) and the lowest solid residue (SR) yield (approx. 9 wt.%). Biocrude oils obtained under N_2 or H_2 exhibited higher energy recovery and better quality (higher H/C ratio, lower O/C ratio, higher HHV, lower TAN, and much lower viscosity and molecular weight) than those obtained under O_2. The oils produced in N_2 or H_2 atmosphere mainly contained phenols and aromatic compounds and showed similar boiling point distributions, while more acids were detected in the oils produced in O_2, which presented the highest mild boiling fractions and the least heavy residue fraction.

Author Contributions: Conceptualization, H.W., X.H., Y.Z. and C.X.; methodology, H.W., Y.J., Y.Z. and C.X.; formal analysis, H.W., Y.J., E.P., X.H., Y.Z. and C.X.; investigation, H.W., Y.J. and E.P.; resources, X.H., Y.Z. and C.X.; writing—original draft preparation, H.W. and Y.J.; writing—review and editing, X.H., Y.Z. and C.X.; supervision, Y.Z. and C.X.; project administration, C.X.; funding acquisition, Y.Z. and C.X. All authors have read and agreed to the published version of the manuscript.

Funding: This research was funded by Canadian NRCan Forest Innovation and OERD Clean Energy programs, as well as by Natural Science and Engineering Research Council of Canada (NSERC).The Funding number of NSERC is RGPIN-2019-05159.

Institutional Review Board Statement: Not applicable.

Informed Consent Statement: Not applicable.

Data Availability Statement: Data will be available upon request.

Acknowledgments: The authors gratefully acknowledge the technical support from NRCan Canmet-MATERIALS corrosion and microscopy labs, and the facilities and support offered by Institute for Chemicals and Fuels from Alternative Resources (ICFAR) at Western University.

Conflicts of Interest: The authors declare no conflict of interest.

Appendix A

Table A1. Detailed chemical compounds identified in the biocrude oil obtained from HTL of pinewood sawdust at 300 °C for 60 min under N_2, H_2, and O_2, respectively, with KOH or H_2SO_4 catalyst.

RT [a] (min)	Compounds Name	Relative Composition by Percent Area					
		KOH-N_2	KOH-H_2	KOH-O_2	H_2SO_4-N_2	H_2SO_4-H_2	H_2SO_4-O_2
3.780	Acetic acid		3.036				
5.967	2-Pentanone, 4-hydroxy-4-methyl-	1.409		1.025	2.917	2.731	0.824
7.700	2-Cyclopenten-1-one, 2-methyl-	0.435					
8.517	1,3-Dioxolane-4-methanol, 2,2-dimethyl-, (S)-	0.468					
8.948	Benzaldehyde		0.640				
9.142	2-Cyclopenten-1-one, 3-methyl-		1.036				
9.527	Phenol		0.658				
9.908	Cyclotetrasiloxane, octamethyl-		0.789				
10.288	2,5-Furandione, dihydro-3-methyl-			0.900			
10.555	2-Cyclopenten-1-one, 2,3-dimethyl-		1.264			0.569	
10.868	DL-Norvaline, N-[(phenylmethoxy)carbonyl]-		0.838				
11.054	Acetophenone	1.284	3.519			1.320	
11.109	Pentanoic acid, 4-oxo-			0.927	25.374	6.830	51.470
11.464	Phenol, 2-methoxy-	4.110	42.040			1.627	
11.959	2-Isopropylbenzenethiol, S-methyl-				2.366		
12.204	N-Chlorocarbonyl-N-methoxy-N-isopropylamine		2.131				
12.284	Pentanoic acid, 2-methyl-4-oxo-						1.155
12.454	Phenol, 2,6-dimethyl-		0.902				
12.919	2-Cyclopenten-1-one, 2,3,4,5-tetramethyl-		0.935				

Table A1. *Cont.*

RT [a] (min)	Compounds Name	Relative Composition by Percent Area					
		KOH-N_2	**KOH-H_2**	**KOH-O_2**	**H_2SO_4-N_2**	**H_2SO_4-H_2**	**H_2SO_4-O_2**
13.028	Benzoic acid			11.585			1.545
13.143	Creosol	2.549	1.818			0.656	
13.232	Catechol		2.648		1.136		
13.341	Butanedioic acid, monopropargyl ester			0.400			
13.460	1H-Benzimidazole, 2-ethyl-		0.723				
13.895	Butanedioic acid, methyl-			0.780			
14.022	4-Nonanol, 4-methyl-			0.615			
14.200	Cyclohexene, 1-methyl-4-(1-methylethylidene)-	0.926	1.700			0.966	
14.230	Naphthalene, 2,6-bis(1,1-dimethylethyl)-				1.404		0.734
14.327	Benzoic acid, 3-methyl-			2.079			
14.420	Phenol, 4-ethyl-2-methoxy-	4.622	2.253	1.428			
14.445	1H-Inden-1-one, 2,3-dihydro-				1.314	1.479	
14.805	1-Methylindan-2-one		1.250	0.869			
15.067	2-Cyclopenten-1-one, 2,3-dimethyl-			0.733	1.958	1.482	
15.113	3-Cyclohexen-1-one, 2-isopropyl-5-methyl-		0.834				0.445
15.210	Hydrocinnamic acid			1.012			0.170
15.325	1,4-Benzenediol, 2-methyl-		0.516				
15.405	1(3H)-Isobenzofuranone			0.891			
15.418	7-Methylindan-1-one	0.370	1.520		1.395	0.484	
15.553	Benzaldehyde, 3-hydroxy-			2.111			
15.629	Phenol, 2-methoxy-4-propyl-	3.286				1.121	
15.963	Benzene, 1-ethenyl-4-methyl-	1.105			0.812	2.971	
16.001	Ethanone, 1-(3-hydroxyphenyl)-		1.363				0.865
16.048	Vanillin	0.578	0.260	5.944	0.508		1.040
16.149	Benzoic acid, 3-(1-methylethyl)-			0.882			
16.293	1H-Inden-1-one, 2,3-dihydro-3,3-dimethyl-	1.203					
16.331	1,2-Diethoxybenzene		0.809	2.494	1.059		0.900
16.412	2-(Cyclohex-1-enyl)-furan					1.896	
16.623	Acetophenone, 4′-hydroxy-			1.674			
16.754	Phenol, 2-methoxy-4-(1-propenyl)-	1.309					
16.792	Benzoic acid, 3-formyl-			1.281			
16.953	3-Ethenylheptan-2,6-dione			0.932			
16.961	Phenol, 2-(1,1-dimethylethyl)-						0.531
17.067	4-Methylphthalaldehyde			0.556			
17.071	1,4-Benzenediamine, N,N,N′,N′-tetramethyl-	1.014					
17.169	1-Tetralone, 8-hydroxy-		0.267				
17.287	Benzoic acid, 4-hydroxy-						0.342
17.355	Apocynin	1.549		10.221			0.470
17.384	Ethyl 3-(2-furyl)propenoate		0.615				
17.782	4-Hydroxy-3-methylacetophenone			0.602			
17.883	2-Cyclopentenecarboxylic acid, 5-hydroxy-5-methyl-2-(1-methylethyl)-, methyl ester, trans-		0.681				
18.175	2-Propanone, 1-(4-hydroxy-3-methoxyphenyl)-	1.637			2.935	0.868	
18.196	1-(4-methylthiophenyl)-2-propanone		1.716				
18.234	Benzenamine, 4-methyl-3-nitro-			0.930			
18.462	4-Acetylbenzoic acid			4.376			
18.648	Phenol, 2-(1,1-dimethylethyl)-4-methyl-			0.509			
18.813	Benzene, 1-methyl-3,5-bis[(trimethylsilyl)oxy]-			2.952			0.223
18.890	4-Hexylphenol, trimethylsilyl ether		1.816				
19.109	4-Ethoxy-3-anisaldehyde			3.261			
19.460	Phthalan		0.563				
19.562	Phenol, 2,6-dimethyl-4-nitro-			0.261			
19.630	Benzofuran, 2,3-dihydro-		0.558				0.477
19.659	1,4-Benzenedicarboxaldehyde, 2-methyl-			0.405			
19.828	Aminosalicylic Acid			0.487			0.218
19.951	Benzene, 1-methoxy-4-(1-methyl-2-propenyl)-	1.820					0.183
19.968	Benzaldehyde, 3-methyl-			1.708			
20.146	Homovanillic acid	1.719					
20.213	Naphthalene, 2-ethoxy-					0.689	
20.315	Ether, bis(p-tert-butylphenyl)			1.287			
20.365	2-Naphthalenol, 3-methoxy-	1.046					
20.391	9-Methyl-3,4-dihydro-2H-pyrido(1,2-a)pyrimidin-2-one		0.465				
20.446	4-Hydroxy-3,5-dimethylbenzoic acid			0.375			
20.496	4,6-Dimethoxy-1-naphthaldehyde					2.105	
20.539	Terephthalic acid			0.226			
20.547	Benzofuran, 2,3-dihydro-2,2,4,6-tetramethyl-	0.965	1.511				
20.695	1,2-Dihydropyrido(3,2,1-kl)phenothiazin-3-one				1.450		
20.704	Butan-1-one, 1-(2,3-dihydro-7,8-dinitro-1,4-benzodioxin-6-yl)-		0.984				
20.962	10H-Phenothiazine, 2-(trifluoromethyl)-				1.202		

Table A1. *Cont.*

RT [a] (min)	Compounds Name	Relative Composition by Percent Area					
		KOH-N_2	KOH-H_2	KOH-O_2	H_2SO_4-N_2	H_2SO_4-H_2	H_2SO_4-O_2
20.983	2-Propenoic acid, 3-(3-hydroxyphenyl)-, methyl ester		0.736				
21.122	5-Hydroxy-1-tetralone		0.553				
21.148	Salicylhydroxamic acid			0.692			
21.258	1,4-Benzenediamine, N,N′-diethyl-			2.026			
21.346	Benzaldehyde, 2-nitro-, diaminomethylidenhydrazone	1.575			1.229		
21.363	Methyleugenol		0.777			1.482	
21.389	2-Methyl-5-nitrobenzoic acid			1.085			
21.397	1H-Benzotriazole-5,6-dicarbonitrile						0.481
21.592	Pyridine, 4-(5-benzo[1,3]dioxol-5-yl-[1,2,4]oxadiazol-3-yl)-			1.139			
21.735	Benzenesulfonic acid, 4-methyl-			0.628			
21.820	4-Methoxycinnamaldehyde					1.680	
21.854	Dihydrofuranno(3,2-f)coumaran	2.134	1.056	1.447			0.584
22.006	4,4′-Stilbenedicarbonitrile					1.748	
22.010	(6,7-Dimethoxy-3,4-dihydro-1-isoquinolinyl)acetonitrile		0.941	1.290	1.385		0.363
22.137	1-[2,2′:5′,2″]Terthiophen-5-yl-ethanone				1.232		
22.209	Benzene, 1-phenyl-4-(2,2-dicyanoethenyl)				1.378		
22.213	Benzo(a)phenazine					1.615	
22.222	Dibenzo[c,h][2,6]naphthyridine						0.481
22.230	2,2′-Bi-1H-indene		1.321				
22.340	1,4-Dimethyl-4,5,7,8-tetrahydroimidazo-[4,5-E]-1,4-diazepin-5,8(6H)-dione		1.538		2.477	2.927	1.088
22.509	2-Ethoxyphenyl isocyanate	1.220		1.912			
22.535	Asarone		0.785		0.977	1.374	0.789
22.683	Tricyclo[4.3.0.0(7,9)]nonane, 2,2,5,5,8,8-hexamethyl-, (1.alpha.,6.beta.,7.alpha.,9.alpha.)-	1.683				0.934	
22.924	Benzaldehyde, 2-methoxy-4-methyl-			0.944			
23.106	6-Acetyl-5-hydroxy-2,7-dimethyl-1,4-naphthoguinone					1.211	
23.135	Benzoic acid, 3-methoxy-			0.643			0.495
23.321	As-Indacene, 1,2,3,6,7,8-hexahydro-1,1,6,6-tetramethyl-4-(1-methylethyl)-					2.247	
23.385	(+)-3-Carene, 2-.alpha.-isopropenyl-	1.063					
23.402	2,2′-Isopropylidenebis(3-methylbenzofuran)				1.837	1.728	
23.579	2,4,5,6-Tetrachloro-nicotinamide				0.587		
23.588	9,10-Dihydro-12H-5-oxabenzocyclodecene-6,11-dione	1.082					
23.596	Fluorene, 2,7-bis(1-hydroxyethyl)-					3.234	
23.681	1,3-Benzodioxole, 4-methoxy-6-(2-propenyl)-						0.287
23.824	[1,2,4]Triazolo[1,5-a]pyrimidine, 6-chloro-2-(2-furanyl)-5,7-dimethyl-	1.299					
23.884	Benzene, 2-ethyl-1,3-dimethyl-					1.862	
23.968	Dithiocarbonic acid, O-ethyl ester, methylene-S(IV)-trifluoromethyl ester	0.689					
24.006	Estra-1,3,5(10)-trien-3-ol					0.564	
24.019	n-Hexadecanoic acid			1.996			1.063
24.159	7-Oxabicyclo[4.1.0]heptane, 1-(2,3-dimethyl-1,3-butadienyl)-2,2,6-trimethyl-, (E)-	0.419					
24.180	1,2-Dimethyl-3-nitro-4-nitroso-benzene			0.532			
24.302	Benzenemethanol, 2-methyl-.alpha.-phenyl-						0.595
24.311	1-Phenanthrenecarboxaldehyde, 1,2,3,4,4a,9,10,10a-octahydro-1,4a-dimethyl-7-(1-methylethyl)-, [1S-(1.alpha.,4a.alpha.,10a.beta.)]-					2.870	
24.412	Methyl 2-hydroxy-4-methoxybenzoate, trimethylsilyl ether	1.238					
24.488	Phenol, 4,4′-methylenebis-			0.412			
24.531	7,8-Dihydro-9H-cyclopenta[a]pyren-9-one				1.256	1.563	0.684
24.552	1,4-Cyclohexanedicarboxylic acid, 2,5-dioxo-, diethyl ester		0.877				
24.704	Ketone, 7-methoxy-2-benzofuranyl methyl					1.641	
24.729	2-Acetyl-3-methylbenzo[b]thiophene		1.523				
24.742	Benzo[b]thiophene, 2,3-diethyl-						0.969
24.801	2,4(1H,3H)-Quinazolinedione, 1,3-diethyl-				0.811		
24.818	1-METHOXY-2-TERT.-BUTYL-4,6-DINITROBENZENE					1.304	
24.962	di-p-Tolylacetylene						0.863
25.118	5-Methoxy-2-naphthalen-2-yl-2H-indazole				0.659		
25.127	Silane, dimethyl(2-naphthoxy)isobutoxy-		0.598				

Table A1. *Cont.*

RT [a] (min)	Compounds Name	Relative Composition by Percent Area					
		KOH-N_2	**KOH-H_2**	**KOH-O_2**	**H_2SO_4-N_2**	**H_2SO_4-H_2**	**H_2SO_4-O_2**
25.199	Homovanillic acid	4.555					
25.211	2,3,6-Trimethoxybenzoic acid						0.723
25.216	Imidazo[1,2-b]-1,2,4-triazine, 6-(3-methoxyphenyl)-2,3-dimethyl-					1.817	
25.372	Androstane-3,17-dione, (5.alpha.)-			0.398	2.705	1.271	1.073
25.385	2,5-Diethyl-3,4-diphenyl cyclopentadienone	1.263	0.974				
25.478	1,2,3,4-Tetrahydrobenz[a]anthracene	1.459				1.355	
25.512	9H-Xanthen-9-one, 1,3-dihydroxy-2-methyl-			0.807			
25.541	3,5-di-tert-Butyl-4-hydroxybenzyl alcohol					1.207	
25.736	Naphthalene, 1-(2-naphthalenyloxy)-	3.021	1.884		4.552		2.427
25.833	cis-Vaccenic acid			9.907			
25.842	4-Methoxyphenol, pentafluoropropionate				2.017		
25.871	2-Hexanone, phenyl(2-propenyl)hydrazone	0.664	0.925				
26.066	Ethyl Oleate	3.889		3.408	4.803	1.827	1.477
26.192	1,2-Epoxy-3,4-dihydroxycyclohexano[a]pyrene, (3s,4s-)						1.911
26.205	2H-1-Benzopyran-3(4H)-one, 8-methoxy-2-(1-naphthalenyl)-, oxime				1.142	0.851	
26.273	3H-Benzo[f]chromen-3-one, 2-(4-methoxyphenyl)-		0.812				
26.328	3,4-Dimethoxychalcone					1.625	
26.450	Benzoic acid, 4,5-dimethoxy-2-(2-phenylethenyl)-				1.794		
26.455	Estra-1,3,5(10)-triene-6,17-dione, 3-hydroxy-					1.055	
26.543	1,3-Cyclohexanedione, 2-[4-(4-methoxyphenylamino)-2-thiazolyl]-	1.047		1.159			
26.590	Retene					2.830	2.305
26.708	Benzene, 1,3-dimethoxy-5-[(1E)-2-phenylethenyl]-	1.780			1.156		
26.713	p-Bis(p-methoxyphenyliminomethyl)benzene				2.831	0.880	
26.806	trans-3′,4′,5′-Trimethoxy-4-(methylthio)chalcone		0.696			2.653	1.466
26.899	1-Benzhydrylazetidin-3-ol						0.574
26.966	2-(((6-Fluoro-4H-1,3-benzodioxin-8-yl)methyl)sulfanyl)-1H-benzimidazole				1.289		
26.975	Benzoic acid, 4,5-dimethoxy-2-(2-phenylethenyl)-					0.877	
26.983	2-Amino-4-azido-5-[3,4,5-trimethoxybenzyl]pyrimidine	0.965					
26.987	3Alpha,5-cyclo-6beta,19-epoxy-5alpha-androstan-17-one						0.663
27.148	Acridin-9-yl-(2,4-dimethoxy-phenyl)-amine	0.979					
27.203	13-(2-Methoxyphenyl)tricyclo[8.2.2.24,7]hexadeca-1(13),4,6,10(14),11,15-hexaene-5-carbaldehyde						2.588
27.254	Estra-1,3,5(10)-trien-17-one, 3-methoxy-					1.301	
27.296	(.+/−.)-Uleine				1.801		
27.322	N,N-Dimethylindoaniline	4.244					
27.457	2-[4-(1,2-Diphenyl-but-1-enyl)-phenoxy]-ethylamine				1.827		
27.461	Benzofuran-5-ol, 3-(2-furanoyl)-4-dimethylaminomethyl-					1.432	
27.567	Homovanillic acid			1.146			
27.571	Ethyl homovanillate	5.919					
27.732	Benzeneacetic acid, 4-hydroxy-3-methoxy-, methyl ester		0.713		2.750	2.782	
27.740	3-Penten-2-one, 4-(2,2,6-trimethyl-7-oxabicyclo[4.1.0]hept-1-yl)-, (E)-	4.038					3.109
27.829	2(1H)-Pyrazinone, 3,5,6-tris(1,1-dimethylethyl)-						0.788
27.931	Pyridine, 2-(phenylethynyl)-				0.556		
27.969	8H-5,12b-(Iminoethano)-1H-phenanthro[3,2-d][1,3]dioxin, 2,3,4,4a,5,6-hexahydro-15-methyl-, [4aR-(4a.alpha.,5.alpha.,12b.alpha.)]-					1.431	
28.146	1-(10-Methylanthracen-9-yl)ethanone			0.522			3.722
28.239	1H-1,2,3,4-Tetrazole-1,5-diamine, N(1)-[(2-ethoxy-3-methoxyphenyl)methyl]-			0.385			
28.243	3-(3-Hydroxy-4-methoxyphenyl)-l-alanine	0.769					
28.315	Benzaldehyde, 2-nitro-, diaminomethylidenhydrazone					1.978	
28.556	Methyl p-(trans-styryl)-trans-cinnamate	1.551					

Table A1. *Cont.*

RT [a] (min)	Compounds Name	Relative Composition by Percent Area					
		KOH-N_2	KOH-H_2	KOH-O_2	H_2SO_4-N_2	H_2SO_4-H_2	H_2SO_4-O_2
28.772	1-.beta.-d-Ribofuranosylpyrazolo[3,4-d]pyrimidin-4(5H)-one	1.052					
29.229	Benzene, 1-methoxy-4-(2-cyano-2-phenylethenyl)	0.661					1.046
29.415	2-(E)-Heptenoic acid, (4S)-4-[(t-butoxycarbonyl-(R)-alanyl)amino]-6-methyl-, ethyl ester					1.102	
29.664	4H-1-Benzopyran-4-one, 5-hydroxy-7-methoxy-2-phenyl-				2.369		1.245
29.685	Dinaphtho[2,1-b:1′,2′-d]furan					2.566	
30.096	4-Methoxy-4′,5′-methylenedioxybiphenyl-2-carboxylic acid	2.098					
30.282	i-Propyl nonadecanoate	1.419					
30.336	2,5-Cyclohexadien-1-one, 4-[[4-(dimethylamino)phenyl]imino]-2,5-dimethyl-						0.674
30.425	Dibenz[a,h]anthracene, 1,2,3,4-tetrahydro-				0.801		0.612
30.455	4H-1-Benzopyran-4-one, 5,7-dimethoxy-2-phenyl-					1.208	
30.540	Benzene, 1-(1,1-dimethylethyl)-3,5-dimethyl-2,4,6-trinitro-				0.547		
30.722	4H-1-Benzopyran-4-one, 5,7-dimethoxy-2-phenyl-				2.505	4.742	2.323
31.309	Dimethyldaidzin						0.944
31.318	3H-1,3,4-Benzotriazepine, 7-chloro-2-(methylamino)-5-phenyl-					3.414	
31.457	4-(1,1-Dimethylallyl)-9-methoxy-7H-furo[3,2-g][1]benzopyran-7-one	2.442					
31.690	Benzothiophen-3(2H)-one, 2-(4-ethoxy-3-methoxybenzylideno)-	0.889					
31.952	Benzaldehyde, 2,4-dihydroxy-		0.633	0.807	4.897	2.024	
31.969	2-Cyclohexen-1-one, 2-methyl-5-(1-methylethenyl)-, O-methyloxime, (+)-	8.108					
32.942	Silane, [[(16.alpha.,17.alpha.)-16,17-epoxyestra-1,3,5(10)-trien-3-yl]oxy]trimethyl-	1.385					

[a] Retention time.

References

1. Kumar, M.; Sun, Y.; Rathour, R.; Pandey, A.; Thakur, I.S.; Tsang, D.C. Algae as potential feedstock for the production of biofuels and value-added products: Opportunities and challenges. *Sci. Total Environ.* **2020**, *716*, 137116. [CrossRef] [PubMed]
2. Ahmad, E.; Jäger, N.; Apfelbacher, A.; Daschner, R.; Hornung, A.; Pant, K. Integrated thermo-catalytic reforming of residual sugarcane bagasse in a laboratory scale reactor. *Fuel Process. Technol.* **2018**, *171*, 277–286. [CrossRef]
3. Osman, A.I.; Hefny, M.; Abdel Maksoud, M.; Elgarahy, A.M.; Rooney, D.W. Recent advances in carbon capture storage and utilisation technologies: A review. *Environ. Chem. Lett.* **2021**, *19*, 797–849. [CrossRef]
4. Zhang, S.; Yang, X.; Zhang, H.; Chu, C.; Zheng, K.; Ju, M.; Liu, L. Liquefaction of biomass and upgrading of bio-oil: A review. *Molecules* **2019**, *24*, 2250. [CrossRef] [PubMed]
5. Antar, M.; Lyu, D.; Nazari, M.; Shah, A.; Zhou, X.; Smith, D.L. Biomass for a sustainable bioeconomy: An overview of world biomass production and utilization. *Renew. Sustain. Energy Rev.* **2021**, *139*, 110691. [CrossRef]
6. Nazari, L.; Xu, C.C.; Ray, M.B. Advanced Technologies (Biological and Thermochemical) for Waste-to-Energy Conversion. In *Green Chemistry and Sustainable Technology Advanced and Emerging Technologies for Resource Recovery*; Springer: Berlin/Heidelberg, Germany, 2021; pp. 55–95.
7. Demirkaya, E.; Dal, O.; Yüksel, A. Liquefaction of waste hazelnut shell by using sub-and supercritical solvents as a reaction medium. *J. Supercrit. Fluids* **2019**, *150*, 11–20. [CrossRef]
8. Cao, L.; Iris, K.; Xiong, X.; Tsang, D.C.; Zhang, S.; Clark, J.H.; Hu, C.; Ng, Y.H.; Shang, J.; Ok, Y.S. Biorenewable hydrogen production through biomass gasification: A review and future prospects. *Environ. Res.* **2020**, *186*, 109547. [CrossRef] [PubMed]
9. Chen, H.; Qiu, W. Key technologies for bioethanol production from lignocellulose. *Biotechnol. Adv.* **2010**, *28*, 556–562. [CrossRef] [PubMed]
10. Pham, T.P.T.; Kaushik, R.; Parshetti, G.K.; Mahmood, R.; Balasubramanian, R. Food waste-to-energy conversion technologies: Current status and future directions. *Waste Manag.* **2015**, *38*, 399–408. [CrossRef] [PubMed]
11. Singh, R.; Krishna, B.B.; Mishra, G.; Kumar, J.; Bhaskar, T. Strategies for selection of thermo-chemical processes for the valorisation of biomass. *Renew. Energy* **2016**, *98*, 226–237. [CrossRef]

12. Seehar, T.H.; Toor, S.S.; Sharma, K.; Nielsen, A.H.; Pedersen, T.H.; Rosendahl, L.A. Influence of process conditions on hydrothermal liquefaction of eucalyptus biomass for biocrude production and investigation of the inorganics distribution. *Sustain. Energy Fuels* **2021**, *5*, 1477–1487. [CrossRef]
13. Weir, A.; del Barco Carrión, A.J.; Queffélec, C.; Bujoli, B.; Chailleux, E.; Uguna, C.; Snape, C.; Airey, G. Renewable binders from waste biomass for road construction: A review on thermochemical conversion technologies and current developments. *Constrcution Build. Mater.* **2022**, *330*, 127076. [CrossRef]
14. Singh, R.; Balagurumurthy, B.; Prakash, A.; Bhaskar, T. Catalytic hydrothermal liquefaction of water hyacinth. *Bioresour. Technol.* **2015**, *178*, 157–165. [CrossRef] [PubMed]
15. Xu, Y.; Li, M. Hydrothermal liquefaction of lignocellulose for value-added products: Mechanism, parameter and production application. *Bioresour. Technol.* **2021**, *342*, 126035. [CrossRef] [PubMed]
16. Mishra, R.K.; Kumar, P.; Mohanty, K. Hydrothermal liquefaction of biomass for bio-crude production: A review on feedstocks, chemical compositions, operating parameters, reaction kinetics, techno-economic study, and life cycle assessment. *Fuel* **2022**, *316*, 123377. [CrossRef]
17. Gollakota, A.; Kishore, N.; Gu, S. A review on hydrothermal liquefaction of biomass. *Renew. Sustain. Energy Rev.* **2018**, *81*, 1378–1392. [CrossRef]
18. Pang, S. Advances in thermochemical conversion of woody biomass to energy, fuels and chemicals. *Biotechnol. Adv.* **2019**, *37*, 589–597. [CrossRef]
19. Nagappan, S.; Bhosale, R.R.; Nguyen, D.D.; Chi, N.T.L.; Ponnusamy, V.K.; Woong, C.S.; Kumar, G. Catalytic hydrothermal liquefaction of biomass into bio-oils and other value-added products–A review. *Fuel* **2021**, *285*, 119053. [CrossRef]
20. Dimitriadis, A.; Bezergianni, S. Hydrothermal liquefaction of various biomass and waste feedstocks for biocrude production: A state of the art review. *Renew. Sustain. Energy Rev.* **2017**, *68*, 113–125. [CrossRef]
21. Cao, L.; Zhang, C.; Hao, S.; Luo, G.; Zhang, S.; Chen, J. Effect of glycerol as co-solvent on yields of bio-oil from rice straw through hydrothermal liquefaction. *Bioresour. Technol.* **2016**, *220*, 471–478. [CrossRef] [PubMed]
22. Cao, L.; Zhang, C.; Chen, H.; Tsang, D.C.; Luo, G.; Zhang, S.; Chen, J. Hydrothermal liquefaction of agricultural and forestry wastes: State-of-the-art review and future prospects. *Bioresour. Technol.* **2017**, *245*, 1184–1193. [CrossRef] [PubMed]
23. Jindal, M.K.; Jha, M.K. Effect of process parameters on hydrothermal liquefaction of waste furniture sawdust for bio-oil production. *RSC Adv.* **2016**, *6*, 41772–41780. [CrossRef]
24. Cheng, S.; D'cruz, I.; Wang, M.; Leitch, M.; Xu, C. Highly efficient liquefaction of woody biomass in hot-compressed alcohol−water co-solvents. *Energy Fuels* **2010**, *24*, 4659–4667. [CrossRef]
25. Ye, L.; Zhang, J.; Zhao, J.; Tu, S. Liquefaction of bamboo shoot shell for the production of polyols. *Bioresour. Technol.* **2014**, *153*, 147–153. [CrossRef] [PubMed]
26. Basar, I.A.; Liu, H.; Carrere, H.; Trably, E.; Eskicioglu, C. A review on key design and operational parameters to optimize and develop hydrothermal liquefaction of biomass for biorefinery applications. *Green Chem.* **2021**, *23*, 1404–1446. [CrossRef]
27. Zhu, Z.; Rosendahl, L.; Toor, S.S.; Chen, G. Optimizing the conditions for hydrothermal liquefaction of barley straw for bio-crude oil production using response surface methodology. *Sci. Total Environ.* **2018**, *630*, 560–569. [CrossRef] [PubMed]
28. Obeid, R.; Smith, N.; Lewis, D.M.; Hall, T.; van Eyk, P. A kinetic model for the hydrothermal liquefaction of microalgae, sewage sludge and pine wood with product characterisation of renewable crude. *Chem. Eng. J.* **2022**, *428*, 131228. [CrossRef]
29. Cheng, F.; Porter, M.D.; Colosi, L.M. Is hydrothermal treatment coupled with carbon capture and storage an energy-producing negative emissions technology? *Energy Convers. Manag.* **2020**, *203*, 112252. [CrossRef]
30. Zhang, Y.; Chen, W.-T. Hydrothermal liquefaction of protein-containing feedstocks. In *Direct Thermochemical Liquefaction for Energy Applications*; Elsevier: Amsterdam, The Netherlands, 2018; pp. 127–168.
31. Yin, S.; Dolan, R.; Harris, M.; Tan, Z. Subcritical hydrothermal liquefaction of cattle manure to bio-oil: Effects of conversion parameters on bio-oil yield and characterization of bio-oil. *Bioresour. Technol.* **2010**, *101*, 3657–3664. [CrossRef] [PubMed]
32. Rahimi, A.; Azarpira, A.; Kim, H.; Ralph, J.; Stahl, S.S. Chemoselective metal-free aerobic alcohol oxidation in lignin. *J. Am. Chem. Soc.* **2013**, *135*, 6415–6418. [CrossRef]
33. Rahimi, A.; Ulbrich, A.; Coon, J.J.; Stahl, S.S. Formic-acid-induced depolymerization of oxidized lignin to aromatics. *Nature* **2014**, *515*, 249–252. [CrossRef] [PubMed]
34. Qian, L.; Zhao, B.; Wang, H.; Bao, G.; Hu, Y.; Xu, C.C.; Long, H. Valorization of the spent catalyst from flue gas denitrogenation by improving bio-oil production from hydrothermal liquefaction of pinewood sawdust. *Fuel* **2022**, *312*, 122804. [CrossRef]
35. Hu, Y.; Gu, Z.; Li, W.; Xu, C.C. Alkali-catalyzed liquefaction of pinewood sawdust in ethanol/water co-solvents. *Biomass Bioenergy* **2020**, *134*, 105485. [CrossRef]
36. Santos, R.V.; Mendes, M.A.; Alexandre, C.; Carrott, M.R.; Rodrigues, A.; Ferreira, A.F. Assessment of Biomass and Biochar of Maritime Pine as a Porous Medium for Water Retention in Soils. *Energies* **2022**, *15*, 5882. [CrossRef]
37. Ravichandran, S.R.; Venkatachalam, C.D.; Sengottian, M.; Sekar, S.; Kandasamy, S.; Subramanian, K.P.R.; Purushothaman, K.; Chandrasekaran, A.L.; Narayanan, M. A review on hydrothermal liquefaction of algal biomass on process parameters, purification and applications. *Fuel* **2022**, *313*, 122679. [CrossRef]
38. Yin, S.; Tan, Z. Hydrothermal liquefaction of cellulose to bio-oil under acidic, neutral and alkaline conditions. *Appl. Energy* **2012**, *92*, 234–239. [CrossRef]

39. Yang, W.; Li, X.; Zhang, D.; Feng, L. Catalytic upgrading of bio-oil in hydrothermal liquefaction of algae major model components over liquid acids. *Energy Convers. Manag.* **2017**, *154*, 336–343. [CrossRef]
40. Huang, S.; Mahmood, N.; Tymchyshyn, M.; Yuan, Z.; Xu, C.C. Reductive de-polymerization of kraft lignin for chemicals and fuels using formic acid as an in-situ hydrogen source. *Bioresour. Technol.* **2014**, *171*, 95–102. [CrossRef] [PubMed]
41. Saber, M.; Nakhshiniev, B.; Yoshikawa, K. A review of production and upgrading of algal bio-oil. *Renew. Sustain. Energy Rev.* **2016**, *58*, 918–930. [CrossRef]
42. Vardon, D.R.; Sharma, B.K.; Blazina, G.V.; Rajagopalan, K.; Strathmann, T.J. Thermochemical conversion of raw and defatted algal biomass via hydrothermal liquefaction and slow pyrolysis. *Bioresour. Technol.* **2012**, *109*, 178–187. [CrossRef]
43. Vardon, D.R.; Sharma, B.; Scott, J.; Yu, G.; Wang, Z.; Schideman, L.; Zhang, Y.; Strathmann, T.J. Chemical properties of biocrude oil from the hydrothermal liquefaction of Spirulina algae, swine manure, and digested anaerobic sludge. *Bioresour. Technol.* **2011**, *102*, 8295–8303. [CrossRef] [PubMed]
44. Mahmood, N.; Yuan, Z.; Schmidt, J.; Xu, C.C. Hydrolytic depolymerization of hydrolysis lignin: Effects of catalysts and solvents. *Bioresour. Technol.* **2015**, *190*, 416–419. [CrossRef]
45. Hao, B.; Xu, D.; Jiang, G.; Sabri, T.A.; Jing, Z.; Guo, Y. Chemical reactions in the hydrothermal liquefaction of biomass and in the catalytic hydrogenation upgrading of biocrude. *Green Chem.* **2021**, *23*, 1562–1583. [CrossRef]
46. Chen, W.-T.; Zhang, Y.; Zhang, J.; Schideman, L.; Yu, G.; Zhang, P.; Minarick, M. Co-liquefaction of swine manure and mixed-culture algal biomass from a wastewater treatment system to produce bio-crude oil. *Appl. Energy* **2014**, *128*, 209–216. [CrossRef]
47. Camus, M.; Condassamy, O.; Ham-Pichavant, F.; Michaud, C.; Mastroianni, S.; Mignani, G.; Grau, E.; Cramail, H.; Grelier, S. Oxidative Depolymerization of Alkaline Lignin from Pinus Pinaster by Oxygen and Air for Value-Added Bio-Sourced Synthons. *Polymers* **2021**, *13*, 3725. [CrossRef]